

# The Trefoil

Joel C. Langer and David A. Singer

**Abstract.** Dixon’s elliptic functions parameterize the real sextic trefoil curve by arc length and the complex curve as an embedded Platonic surface with 18 (or 108) faces.

**Mathematics Subject Classification (2010).** 14H45, 14H50, 14H52, 33E05.

**Keywords.** Algebraic curve, elliptic function, Platonic surface.

## 1. Introduction

The purpose of this paper is to give a detailed description of the *trefoil*, a sextic curve whose exceptional properties set it apart from other algebraic plane curves of low degree. The trefoil  $\mathcal{T}$  has polar equation  $r^3 = 2A \cos(3\theta)$  and is given by  $(x^2 + y^2)^3 = A(2x^3 - 6xy^2)$ , in rectangular coordinates. (Except once in §9, we will use  $A = 1$ .)

Arc length parameterization of  $\mathcal{T}$  will be simply expressed in terms of certain elliptic functions known as *Dixon functions*. This is already unusual, for no other elliptic curve  $f(x, y) = 0$  of low degree ( $d < 8$ ) can be so parameterized by elliptic functions [18]; allowing genus zero, only the Bernoulli lemniscate has such unit speed parameterization [12].

Further, the arc length parameterization of the trefoil will be shown to be equivariant with respect to a 54-element symmetry group of the underlying elliptic curve and corresponding projective symmetry group  $\text{Sym}(\mathcal{T}) \subset \text{PGL}(3, \mathbb{C})$  (Theorem 1).

In this sense, arc length parameterization provides the trefoil’s structure as a genus 1 *Platonic surface*, whose 18 equilateral-triangular faces may be arbitrarily exchanged and rotated, like the faces of an icosahedron.

This too is reminiscent of the Bernoulli lemniscate; however, it is a rational parameterization which realizes the lemniscate’s octahedral group of projective symmetries [15] (while its arc length parameterization has a smaller symmetry group [16]).

The existence of arc length parameterizations by elliptic functions is also of algebraic and number-theoretic significance for these curves. Indeed, the lemniscate

and trefoil are among only a handful of curves known to satisfy uniform subdivision theorems.

The classical result of Gauss and Lambert asserts that the regular  $n$ -gon may be constructed by straightedge and compass if and only if  $n = 2^j p_1 \dots p_k$  is a power of two times a product of distinct Fermat primes  $p = 2^{2^m} + 1$ . Similarly, Abel showed that the Bernoulli lemniscate could be uniformly subdivided for precisely the same integers  $n$ . Both results may be said to belong to the province of Galois theory; while the former result is built on the angle addition identities for the circular functions  $\sin s$ ,  $\cos s$ , Abel's deeper result depends on identities for the lemniscate elliptic functions  $\operatorname{sl} s$ ,  $\operatorname{cl} s$ ,  $\operatorname{dl} s$  and the existence of complex multiplication on the underlying elliptic curve [21], [20].

Likewise, the result of Cox and Shurman [8] on uniform subdivision of the ( $12^{\text{th}}$ -degree) *clover*—by extraction of square roots and cube roots, under number-theoretic conditions involving Pierpont primes—is built on the third *clover function*  $\varphi_3(x)$  (which arises directly from the elliptic arc length integral for clovers). The corresponding result was shown to hold for the trefoil [17], again using  $\varphi_3(x)$ .

Presently, the Dixon functions and the trefoil turn out to be a perfect fit. Since these functions are not very well known, we will provide some background. In particular, we present a number of relevant identities and apply them first to the *Fermat cubic*  $x^3 + y^3 = 1$ , a simpler curve with the same group of projective symmetries as  $\mathcal{T}$ .

The trefoil and its parameterization will then be obtained from the latter non-singular cubic via *quadratic transformation*, which turns the cubic's nine inflection points into three triple points of  $\mathcal{T}$  while preserving all symmetries. Though identical as a Riemann surface, the resulting sextic  $\mathcal{T}$  thereby acquires precisely the necessary (highly inflectional) behavior at its ideal triple points to be meromorphically parameterizable by arc length. Once again, this parallels the case of the lemniscate (a *triflectional* quartic obtained by inversion of a quadric).

To conclude this introduction, Figure 1 illustrates several of the trefoil's noteworthy features:

1. Unit speed parameterization  $\gamma(s) = x(s) + iy(s)$  of  $\mathcal{T}$  (red) extends meromorphically to all  $\zeta = s + it \in \mathbb{C}$ .  $\mathcal{T}$  has foci at the cube roots of unity  $1$ ,  $\omega = e^{2\pi i/3}$ ,  $\omega^2$ . Removing 'focal rays'  $[\omega^j, \infty)$ , the *curvilinear tiling* on the remaining domain is the conformal,  $\gamma$ -image of a (standardly tiled) hexagon. Odd vertices are simple poles  $\gamma(v_{2j+1}) = \infty$ , and even vertices are mapped to foci,  $\gamma(v_{2j}) = \omega^j$ , where angles are tripled.
2.  $\gamma : \mathbb{C} \rightarrow S^2$  defines time-periodic evolution of closed curves in the Riemann sphere  $S^2 = \mathbb{C} \cup \{\infty\}$ ; ignoring tile colorings, the figure is simply the (many-to-one)  $\gamma$ -image of a family of horizontal lines. *Evolved curves*  $u \mapsto \gamma_j(u) = \gamma(u + it_j)$  are shown for uniformly spaced 'times'  $t_0 = 0, \dots, t_{12}$ ; in particular,  $\gamma_0 = \gamma_{12}$  is the (real) trefoil,  $\gamma_4$  is the *trihyperbola*—the inverse of  $\mathcal{T}$  in the unit circle  $\gamma_8$ . The remaining curves belong to a continuous family  $\gamma_t$  of algebraic

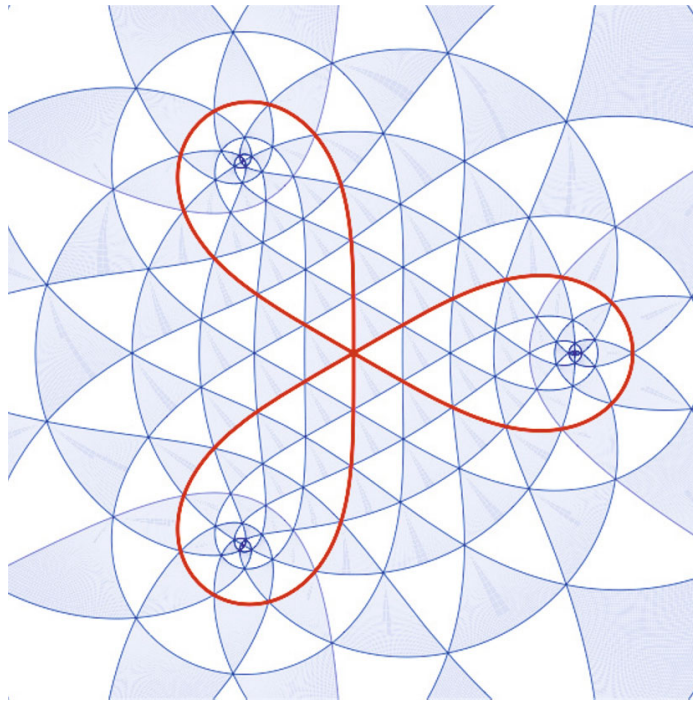


FIGURE 1. The trefoil family of sextics  $\gamma(u + it_j)$ .

- curves of degree *six* [18]. ( $\gamma_t$  represents a *closed geodesic* in a symmetric space geometry of analytic curves [4], [5].)
3. The discrete family of curves  $\{\gamma_j\}$ ,  $j = 0, \dots, 11$ , subdivide the real trefoil  $\gamma_0$  into 36 arcs of equal length. The subdivision points, like all intersection points  $z = x + iy$  in the figure, have algebraic coordinates; in fact,  $x$  and  $y$  can be expressed via square roots, cube roots and rational operations.
  4.  $\gamma(\zeta)$  defines a three-to-one branched covering of the Riemann sphere  $S^2$  by a torus  $T^2$ , ramified over foci  $\omega^j$ . Namely, each point  $z \neq 1, \omega, \omega^2$  is a point of threefold ( $60^\circ$ ) intersection of arcs  $z \in \gamma_{t_1} \cap \gamma_{t_2} \cap \gamma_{t_3}$ . The torus is abstractly  $T^2 \simeq \mathbb{C}/\mathbb{Z}[\omega]$  (quotient of  $\mathbb{C}$  by Eisenstein integers).
  5. The curves  $\gamma_t$  may be described as images of parallel geodesics of the elliptic curve  $\mathcal{T} \simeq \mathbb{C}/\mathbb{Z}[\omega]$  under *isotropic projection*. In fact, the complex trefoil may be parameterized by isotropic coordinates according to:  $(x + iy, x - iy) = (\gamma(\zeta), \gamma(-\zeta)) \subset \mathbb{C}^2$ . Taking the first coordinate  $\gamma(\zeta)$  corresponds to (complex) linear projection from one of the trefoil's two ideal triple points, the three branches of which project to foci.

## 2. Dixon's elliptic functions

Elliptic functions were discovered by Niels Henrik Abel, who defined them as inverse functions of elliptic integrals of the first kind. The theory of elliptic functions was

developed by Carl Gustav Jacobi, who introduced the Jacobi Elliptic Functions  $\operatorname{sn} u, \operatorname{cn} u, \operatorname{dn} u$  in 1829; these functions are adapted to quartic elliptic curves

$$y^2 = (1 - x^2)(1 - k^2 x^2).$$

(The lemniscate arc length leads to the case  $k = i$ .)

Later, Karl Weierstrass developed the theory using what are now known as the Weierstrass  $\wp$  functions; these naturally parametrize cubics in the Weierstrass form

$$y^2 = 4x^3 - g_2x - g_3.$$

The Dixon elliptic functions, which first appeared in 1890 [9], are based on the curves

$$x^3 + y^3 - 3axy = 1.$$

We are interested in the case of the Fermat cubic,  $a = 0$ , for which the functions display a special hexagonal symmetry. (As indicated in §10, this is the case  $g_2 = 0$  in the Weierstrass theory, the other distinguished case,  $g_3 = 0$ , being that of the lemniscate.)

Indeed, the *Dixonian sine*  $\operatorname{sm} z$  can be used to map a regular hexagon onto the Riemann sphere; the hexagon interior is mapped conformally onto the complement of the three rays joining  $\infty$  to a cube root of unity. The equation  $\operatorname{sm} z = \tan \frac{p}{2} e^{i\lambda}$  associates the point in the hexagon with complex coordinate  $z = x + iy$  with the point in the sphere with latitude  $\pi/2 - p$  and longitude  $\lambda$ . This accounts for the extensive investigation of the case  $a = 0$  in a work on geodesy [2] (see pp. 68–75).

Aside from the old references [9] and [2], there appears not to be much literature on the Dixon functions *per se*. However, much more recently, these functions were singled out as functions of special interest in combinatorics and probability because of the unusual continued fraction expansions of related Laplace transforms [7].

The function  $w = \operatorname{sm} z$  is implicitly defined for real  $z$  by the equation

$$z = \int_0^w \frac{dx}{(1 - x^3)^{2/3}}, \quad (2.1)$$

and  $\operatorname{cm} z$  is subsequently defined by the relation

$$\operatorname{sm}^3 z + \operatorname{cm}^3 z = 1. \quad (2.2)$$

Then  $\operatorname{sm}(0) = 0$ ,  $\operatorname{cm}(0) = 1$ , and

$$\frac{d}{dz} \operatorname{sm} z = \operatorname{cm}^2 z, \quad \frac{d}{dz} \operatorname{cm} z = -\operatorname{sm}^2 z. \quad (2.3)$$

Indeed, this first order system may be used to define  $\operatorname{sm} z$  and  $\operatorname{cm} z$  (and serves as the starting point for the theory developed in [7]).

We note that the above integral is the case  $n = 3$  of the integral  $z = \int_0^w \frac{dx}{(1 - x^n)^{2/n}}$  considered in 1864 by H. A. Schwarz. Along the circle  $w = e^{i\theta}$ , the integral has derivative  $\frac{dz}{d\theta} = \frac{ie^{i\theta}}{(1 - e^{in\theta})^{2/n}} = \frac{i}{(-2i \sin \frac{n\theta}{2})^{2/n}}$ ; so  $\arg(z'(\theta))$  is piecewise constant,

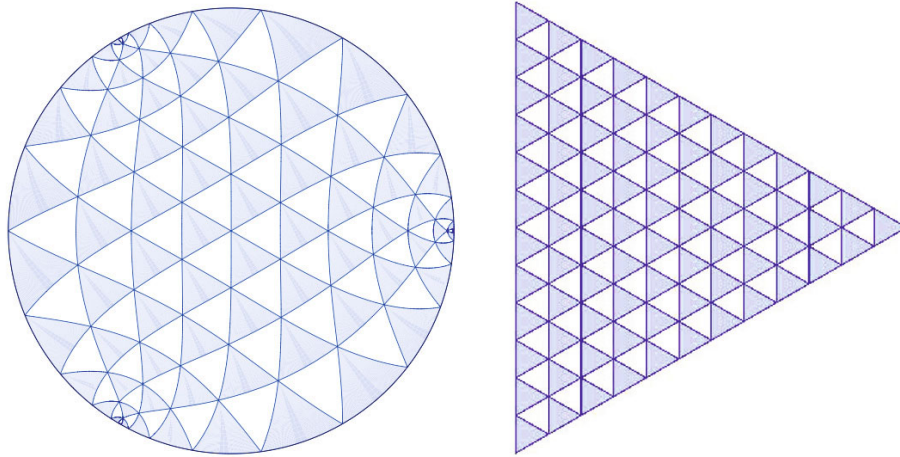


FIGURE 2. Conformal mapping from disk to triangle.

with jumps at zeros of  $\sin n\theta/2$ . It then follows by complex function theory that  $w \mapsto z$  defines a conformal mapping of the unit disc onto a regular  $n$ -gon.

Figure 2 shows the mapping in the (exceptionally nice) case  $n = 3$ . The inverse mapping  $w = \text{sm } z$  is initially defined on a triangular tile, which  $\text{sm}$  maps to the disk; but the Schwarz symmetry principle allows one to extend  $\text{sm}$  to map an adjacent tile to the exterior of the disc. Iterating the procedure, one obtains a doubly periodic, meromorphic function on the complex plane, whose symmetry properties may be understood in terms of the standard tiling by equilateral triangles.

Corresponding arguments apply to the case  $n = 4$ , the *lemniscate sine*  $\text{sl } z$  and associated square tiling. It happens that such mapping properties were not understood until after the lemniscate integral had already played a major role in the development of elliptic integrals.

Oddly, it was not until 1882 that Cayley [6] explicitly identified the above map  $w \mapsto z$  (2.1) as an elliptic integral, thus paving the way for the development of the formal properties of  $\text{sm } z$  and  $\text{cm } z$  as elliptic functions.

To be more specific, let

$$K = \int_0^1 \frac{dx}{(1-x^3)^{2/3}} = \frac{1}{3} \frac{(\Gamma(\frac{1}{3}))^2}{\Gamma(\frac{2}{3})} = 1.76663875\dots,$$

Here, the substitution  $t = x^3$  yields  $K$  in terms of a beta function,  $K = \frac{1}{3} B(\frac{1}{3}, \frac{1}{3})$ , consequently in terms of the gamma function  $\Gamma(x)$  by Binet's formula ([22], p.204). Then  $\text{sm } z$  and  $\text{cm } z$  have periods  $p_1 = 3K$  and  $p_2 = 3\omega K$ , where  $\omega = \frac{-1+i\sqrt{3}}{2}$  is a cube root of unity:

$$\text{sm}(z + 3\omega^j K) = \text{sm } z, \quad \text{cm}(z + 3\omega^j K) = \text{cm } z, \quad j = 0, 1, 2 \quad (2.4)$$

(Of course  $p_3 = 3\omega^2 K$  is not independent;  $p_1 + p_2 + p_3 = 0$ .)

As for any elliptic functions, one can describe the values of  $\operatorname{sm} z$  and  $\operatorname{cm} z$ ,  $z \in \mathbb{C}$ , via a tiling of the plane by copies of a ‘period parallelogram’  $P$  whose edges corresponding to the pair of periods. Alternatively, these functions are well-defined on the torus  $\Sigma = \mathbb{C}/\Pi$  defined as the quotient of  $\mathbb{C}$  by the lattice of periods  $\Pi = \{jp_1 + kp_2\}$ . Thus, e.g., the parameterization (2.2) identifies the Fermat cubic as an elliptic curve; topologically, the curve is a torus obtained from  $P$  with opposite edges identified via  $p_1$  and  $p_2$ .

However, this elliptic curve is exceptional: The lattice  $\Pi$ —a scaling of the Eisenstein integers  $\mathbb{Z}[\omega]$ —is *hexagonal*. The special  $120^\circ$ -rotational symmetry of the lattice,  $\omega\Pi = \Pi$ , is crucial for all that follows.

To discuss this symmetry in terms of the elliptic functions  $\operatorname{sm} z$  and  $\operatorname{cm} z$ , observe that the substitution  $x \mapsto \omega x$  results in multiplication of the integral (2.1) by  $\omega$ , and the corresponding symmetry follows for the inverse function  $\operatorname{sm} z$ . In fact, we have the identities,

$$\operatorname{sm}(\omega z) = \omega \operatorname{sm} z, \quad \operatorname{cm}(\omega z) = \operatorname{cm} z, \tag{2.5}$$

which correspond to  $\operatorname{sm} z = \sum_{n=0}^\infty a_n z^n$  having only powers of  $z$  of order  $3k + 1$  and  $\operatorname{cm} z$  having only powers of  $z^3$ .

Incidentally, this yields the second period as an immediate consequence of the first:  $\operatorname{sm}(z + 3\omega K) = \omega \operatorname{sm}(\omega^2 z + 3K) = \omega \operatorname{sm}(\omega^2 z) = \operatorname{sm} z$  and likewise for  $\operatorname{cm} z$ .

### 3. The Eighteen (or 108) Triangles of $\Sigma$

To make a musical analogy: If a doubly periodic function *repeats* on each translate of a period parallelogram  $P$ , it may be said to *repeat with variation* on subtiles of  $P$ . This applies to  $\operatorname{sm} z$  and  $\operatorname{cm} z$  *con forza!*

Consider the *lattice of inflections*  $\Lambda = \{(j + k\omega)K\}$ —the set of zeros and poles of  $\operatorname{sm}'' z$  or  $\operatorname{cm}'' z$  (see also Remark 5.2). There is a corresponding triangulation of  $P$  by 18 equilateral triangles. Figure 3 (left) shows (red, white, blue) points of  $\Lambda$  and the triangulated  $P$ .

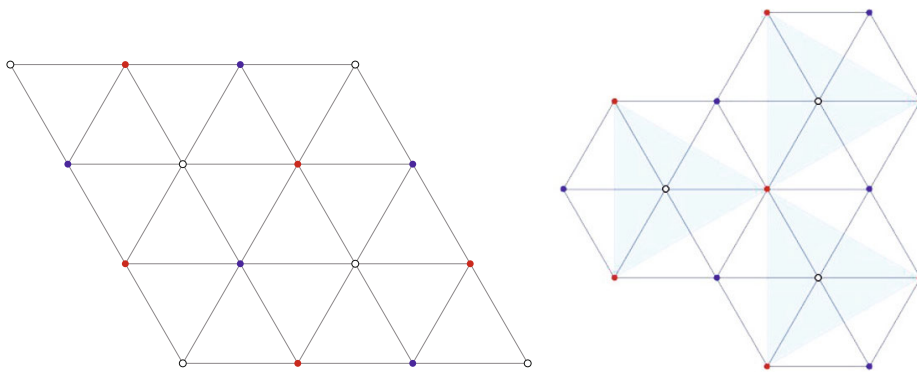


FIGURE 3. Lattice  $\Lambda$ ;  $P$  and  $H$  domains for  $\operatorname{sm} z$ .

Some of the relevant identities for  $\operatorname{sm} z$  and  $\operatorname{cm} z$  do not appear in [2] or [9], but follow easily from the addition formulas (see §10). To begin,  $\operatorname{sm} z$ ,  $\operatorname{cm} z$  vary under  $\Lambda$ -translations via reciprocals and quotients:

$$\operatorname{sm}(z + \omega^j K) = \frac{\omega^j}{\operatorname{cm} z}, \quad \operatorname{cm}(z + \omega^j K) = -\frac{\operatorname{sm} z}{\omega^j \operatorname{cm} z}, \quad j = 0, 1, 2 \quad (3.1)$$

One recovers Equation 2.4 as the third iterate of Equation 3.1.

Likewise, one may refine the rotational symmetry; in fact, denoting sixth root of unity  $\alpha = \frac{1+i\sqrt{3}}{2} = 1 + \omega = -\omega^2$ , we have

$$\operatorname{sm}(\alpha z) = \frac{\alpha \operatorname{sm} z}{\operatorname{cm} z}, \quad \operatorname{cm}(\alpha z) = \frac{1}{\operatorname{cm} z} \quad (3.2)$$

Thus, in Equations 2.4, one may replace  $\omega$  by  $\alpha$ . Also, one has

$$\operatorname{sm}(-z) = -\frac{\operatorname{sm} z}{\operatorname{cm} z}, \quad \operatorname{cm}(-z) = \frac{1}{\operatorname{cm} z}, \quad (3.3)$$

the third iterates of Equations 3.2.

Subsequently, one obtains translational symmetries

$$\operatorname{sm}(z + \alpha K) = \frac{\operatorname{cm} z}{\alpha \operatorname{sm} z}, \quad \operatorname{cm}(z + \alpha K) = \frac{-\alpha}{\operatorname{sm} z}, \quad (3.4)$$

as well as formulas for translation by ‘quasi-periods’  $f_{\pm} = \sqrt{3}e^{\pm i\pi/6}K$ :

$$\operatorname{sm}(z + f_+) = \omega \operatorname{sm} z, \quad \operatorname{cm}(z + f_+) = \omega^2 \operatorname{cm} z \quad (3.5)$$

$$\operatorname{sm}(z + f_-) = \omega^2 \operatorname{sm} z, \quad \operatorname{cm}(z + f_-) = \omega \operatorname{cm} z, \quad (3.6)$$

which follow using  $f_{\pm} = (1 \pm \alpha)K$ .

We note that the *lattice of quasiperiods*  $\Lambda_q = \{j f_+ + k f_-\} \subset \Lambda$  may also be described as the set of zeros of  $\operatorname{sm} z$ —white points in Figure 3. Likewise, poles of  $\operatorname{sm} z$  (and  $\operatorname{cm} z$ ) are the (blue) points  $\alpha K + \Lambda_q$ , and (red) points  $K + \Lambda_q$  are all the preimages of 1,  $\omega$  and  $\omega^2$  (zeros of  $\operatorname{cm} z$ ).

We are now in a position to describe the mapping properties of  $\operatorname{sm} z$ . For this purpose, it is helpful to refer to the *trihexagon*  $H = H_0 \cup H_1 \cup H_2$  in Figure 3 (right), which is simply a rearrangement of the triangular tiles of  $P$  and may be used in its place as fundamental region. For concreteness, let the origin be the center of the left hexagonal unit  $H_0$  in the trihexagon.

Now  $\operatorname{sm} z$  maps the (blue) triangle with vertices  $K, \omega K$  and  $\omega^2 K$  conformally onto the unit disk, preserving symmetry ( $\operatorname{sm} 0 = 0$ ,  $\operatorname{sm} \omega^j K = \omega^j$ ). Further, the three 30-120-30-triangles making up the rest of  $H_0$  are mapped onto the exterior of the unit disk (including  $\infty$ ), in accordance with the Schwarz symmetry principle.

Next,  $\operatorname{sm} z$  is extended from  $H_0$  to  $H_1$  and  $H_2$  by quasiperiodicity (3.5, 3.6); say, on  $H_j$  the required rotation of  $w = \operatorname{sm} z$  is  $\omega^j$ . Finally, the entire plane may be tiled by trihexagons, as in Figure 4, and  $\operatorname{sm} z$  is determined on all of these by periodicity (2.4).

Equivalently, a trihexagon may be taken as the model for the elliptic curve  $\Sigma = \mathbb{C}/\Pi$ , and  $\operatorname{sm} z$  may be regarded as a branched triple cover of the Riemann

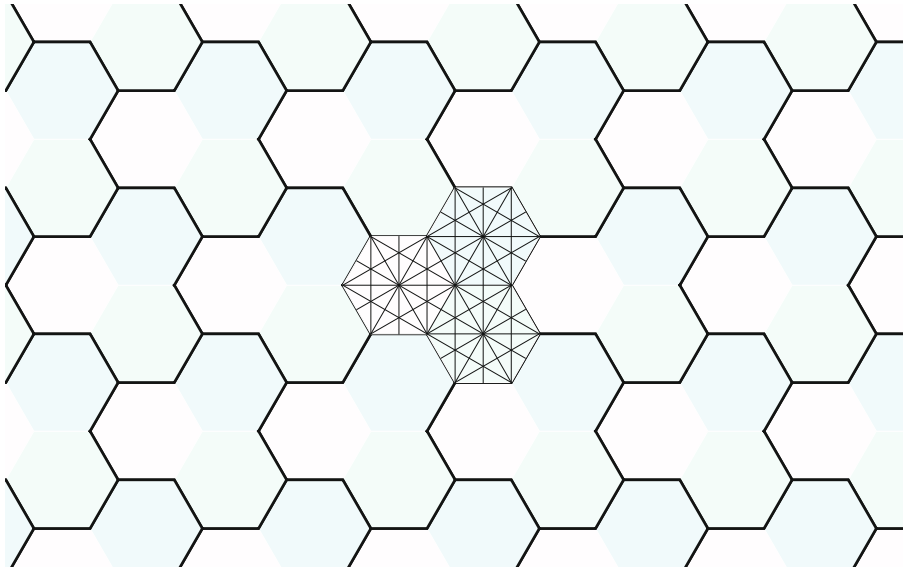


FIGURE 4. Tiling the plane by trihexagons; subdivision of a tile into 108 subtiles (30-60-90 triangles).

sphere by the torus; the behavior of  $sm : \Sigma \rightarrow \hat{\mathbb{C}}$  is now fully understood in terms of just one of the eighteen triangles comprising  $\Sigma$ .

*Remark 3.1.* As discussed in §9, one may further subdivide  $H$  into 108 triangles (Figure 4) such that the values of  $sm z$  on any one determines  $sm z$  on all of  $\mathbb{C}$  by antiholomorphic reflexion!

#### 4. $\Sigma$ as a Platonic Surface

The symmetries of  $sm z$  and  $cm z$  lead us to consider the Riemann surface  $\Sigma$  with extra structure. Namely, the 9 ‘vertices’ of  $\Lambda/\Pi$  determine 9 geodesics (with respect to the flat metric on  $\Sigma = \mathbb{C}/\{jp_1 + kp_2\}$ ), which divide  $\Sigma$  into 18 equilateral triangular faces with edges of length  $K$ . We write  $\Sigma_{18}$  to denote this triangulated Riemann surface.

As for any Riemann surface, the full group of automorphisms of  $\Sigma$  includes a two-parameter abelian subgroup of *translations* identifiable with the additive group  $\Sigma$  itself.  $\text{Aut}(\Sigma)$  also contains the cyclic subgroup of *rotations* about the origin, which may be identified with  $\{\alpha^j\}_{j=1}^6 \simeq \mathbb{Z}_6$ . Then  $\text{Aut}(\Sigma) \simeq \Sigma \rtimes \mathbb{Z}_6$ .

On the other hand,  $\text{Aut}(\Sigma_{18}) \subset \text{Aut}(\Sigma)$  is finite since it must preserve the triangulation. It is in fact the 54-element group  $\text{Aut}(\Sigma_{18}) \simeq \mathbb{Z}_3^2 \rtimes \mathbb{Z}_6$ . There are other useful ways of describing the group  $\text{Aut}(\Sigma_{18})$ . For the moment, we note that  $\mathbb{Z}_3^2$  acts transitively on vertices and therefore  $\text{Aut}(\Sigma_{18})$  acts transitively on oriented edges. Another way of saying the same thing: Any face may be taken to any other, and also may be rotated by multiples of  $120^\circ$ .

In this sense,  $\Sigma_{18}$  abstractly resembles one of the Platonic polyhedra—say, an icosahedron—but is topologically a torus rather than a sphere. Such abstract *Platonic surfaces* have been investigated extensively in recent years, and have been classified for all cases of low genus (where ‘low’ means rather high!). The systematic development of the subject begins with the purely combinatorial notion of *regular map*; we prefer the more descriptive terms *Platonic map*, *Platonic surface*, etc., advocated in the comprehensive investigation [11].

To relate  $\text{Aut}(\Sigma_{18})$  with Dixon function symmetries, we note that factors  $\mathbb{Z}_3^2$  and  $\mathbb{Z}_6$  correspond, respectively, to Equations 3.1 and 3.2. To be more explicit, consider the following linear functions on  $\mathbb{C}$ :  $Az = \alpha z$ , and  $T_j z = z + \omega^j K$ ,  $j = 0, 1, 2$ . Using the same notations for the induced maps on  $\Sigma_{18}$ , we make the identifications  $\mathbb{Z}_6 = \{A^k\}_{k=0}^6$  and  $\mathbb{Z}_3^2 = \{T_0^j T_1^k\}$ , where  $0 \leq j, k \leq 2$ .

The corresponding actions on complex functions  $w = f(z)$  are given by pull-back:

$$A^* f(z) = f(\alpha z), \quad T_j^* f(z) = f(z + \omega^j K) \quad (4.1)$$

In the setting of projective algebraic curves, such ‘symmetries with variation’ for sm, cm presently become full-fledged symmetries for the curves they parameterize.

## 5. Symmetries of the Fermat Cubic

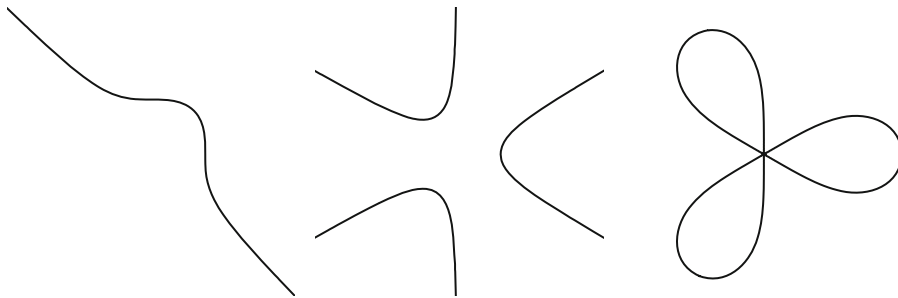


FIGURE 5. From left: Fermat cubic  $x^3 + y^3 = 1$ , trihyperbola  $2x^3 - 6xy^2 = 1$ , trefoil  $(x^2 + y^2)^3 = 2x^3 - 6xy^2$ .

The Dixon functions are well-suited for parameterizing any of the three related curves shown in Figure 5. These are all elliptic curves and turn out to have the same group of projective symmetries. The three curves may also be considered equivalent number theoretically; their coordinates are rationally related.

We begin with the Fermat curve  $\mathcal{F}: x^3 + y^3 = 1$ . For  $u \in \mathbb{R}$ ,  $\gamma(u) = (x(u), y(u)) = (\text{cm } u, \text{sm } u)$  gives a non-singular parameterization of this ‘cubic circle’; note  $\gamma'(u) = (-\text{sm}^2 u, \text{cm}^2 u)$  does not vanish.

*Remark 5.1.* The argument  $u$  in  $\gamma(u)$  has an elegantly simple geometric meaning (as observed by Dixon [9], p. 175). Namely, the area swept out by the ray  $\vec{\gamma}(\mu)$ ,  $0 \leq$

$\mu \leq u$  (see Figure 6) is given by:

$$A(u) = \frac{1}{2} \int_0^u xdy - ydx = \frac{1}{2} \int_0^u \text{cm}^3 \mu + \text{sm}^3 \mu \, d\mu = \frac{u}{2}$$

Thus,  $u$  plays precisely the same role for  $\mathcal{F}$  as the angle  $\theta$  plays for the unit circle—one could say, by precisely the same argument! Or, to give the result a more dynamical interpretation,  $u$  is like *time* in Kepler’s second law of planetary motion. Thus, we take the liberty to proclaim

**Dixon’s Law:** *The line from the origin to  $\gamma(u) = (\text{cm } u, \text{sm } u) \in \mathcal{F}$  sweeps out equal areas in equal increments of time  $\Delta u$ .*

Below, when the Dixon functions  $\text{sm } s, \text{cm } s$  are used to parameterize the trefoil  $\mathcal{T}$ , the argument  $s$  will play instead the role of arc length parameter—see Theorem 9.1 i). The result on uniform divisibility of  $\mathcal{T}$  by arc length [17] will translate to a corresponding result on subdivision of the region  $x^3 + y^3 \leq 1, x \geq 0, y \geq 0$  into  $n$  sectors of equal area  $A(K/n) = K/2n$ . The subdivision is illustrated in Figure 6 for  $n = 17$ .

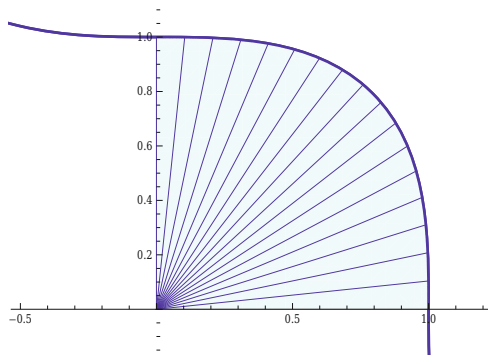


FIGURE 6. Subdivision of the Fermat cubic’s first quadrant into  $n = 17$  sectors of area  $A = K/2n$ .

To discuss projective symmetries of  $\mathcal{F}$ , we consider the complex projective plane:  $\mathbb{C}P^2 = \{[X, Y, Z]\}$ , where  $X, Y, Z$  do not vanish simultaneously and  $[X, Y, Z] \equiv [\lambda X, \lambda Y, \lambda Z]$  for any multiplier  $\lambda \in \mathbb{C} \setminus \{0\}$ . Then elements of the projective group  $\text{PGL}(3, \mathbb{C})$  are represented by non-singular  $3 \times 3$  matrices  $M$ , where  $M \equiv \lambda M$ .

Convenient homogeneous coordinates for  $\mathcal{F}$  are  $x = \alpha X/Z, y = \alpha Y/Z, \alpha = e^{i\pi/3}$ . The resulting equation  $X^3 + Y^3 + Z^3 = 0$  is preserved by permutation of coordinates and multiplication of a coordinate by a cube root of unity  $\omega^j$ . In fact, the group of 54 projective symmetries of the Fermat cubic  $\text{Sym}(\mathcal{F}) \subset \text{PGL}(3, \mathbb{C})$  is generated by the latter two types of symmetries.

Namely,  $\text{Sym}(\mathcal{F})$  contains a subgroup of diagonal matrices  $M = \text{diag}(\omega^j, \omega^k, 1)$ ,  $0 \leq j, k \leq 2$ , with diagonal coefficients chosen from  $1, \omega, \omega^2$  (normalized to have last entry 1); this subgroup is identified with the nine-element abelian group  $\mathbb{Z}_3^2$ . There is also the subgroup of permutation matrices—nonsingular matrices formed with

three ones and six zeros—which may be identified with the six-element symmetric group  $S_3$ . This subgroup complements the first, which is normal in  $\text{Sym}(\mathcal{F})$ : in fact,  $\text{Sym}(\mathcal{F})$  is the 54-element group naturally presented as a semi-direct product:  $\text{Sym}(\mathcal{F}) = \mathbb{Z}_3^2 \rtimes S_3$ .

$\text{Sym}(\mathcal{F})$  is in fact isomorphic to the earlier-defined symmetry group  $\text{Aut}(\Sigma_{18}) = \mathbb{Z}_3^2 \rtimes \mathbb{Z}_6$ , and the isomorphism is realized by the parameterization of the Fermat cubic by Dixon functions,

$$X(z) = \text{cm } z, \quad Y(z) = \text{sm } z, \quad Z(z) = \alpha \quad (5.1)$$

For real values of the parameter  $z = u \in \mathbb{R}$ ,  $p = [X, Y, Z]$  gives a non-singular parameterization of the real locus of  $X^3 + Y^3 + Z^3 = 0$ . Further,  $p(u)$  extends meromorphically to  $\mathbb{C}$  and, by virtue of Equation 2.4, determines a well-defined map  $p : \Sigma \rightarrow \mathcal{F} \subset \mathbb{CP}^2$  (where the values of  $p$  at the common poles of  $\text{cm } z$ ,  $\text{sm } z$  are represented as  $p = [1, \text{sm } z / \text{cm } z, 0]|_{z=\alpha\omega^j K} = [1, \alpha\omega^j, 0]$ ).

To check that  $p$  intertwines the actions of the two symmetry groups  $\text{Aut}(\Sigma_{18})$  and  $\text{Sym}(\mathcal{F})$ , it suffices to consider  $A$  and  $T_1$  (see Equation 4.1), since these two maps generate  $\text{Aut}(\Sigma_{18})$ . Using the abbreviations  $c = \text{cm } z$ ,  $s = \text{sm } z$ , Equation 3.2 gives  $A^*p = [A^*c, A^*s, \alpha] = [1/c, \alpha s/c, \alpha] = [1/\alpha, s, c] = [\omega^2\alpha, s, c] = \text{diag}(\omega^2, 1, 1)M_{13}p$ , where  $M_{13} \in \text{Sym}(\mathcal{F})$  is the permutation matrix which swaps first and third components. Likewise, Equation 3.1 gives  $T_1^*p = [-s/(\omega c), \omega/c, \alpha] = [s, \alpha, c] = M_{123}p$ , where  $M_{123} \in \text{Sym}(\mathcal{F})$  is cyclic permutation. It follows that for each  $g \in \text{Aut}(\Sigma_{18})$ , there is a well-defined  $M_g \in \text{Sym}(\mathcal{F})$  such that the intertwining formula  $pg = M_g p$  holds.

*Remark 5.2.* A non-singular cubic has nine inflection points. In the Hesse normal form,  $p_\lambda = X^3 + Y^3 + Z^3 + \lambda XYZ = 0$ ,  $\lambda^3 + 27 \neq 0$  (essentially the one Dixon used), the nine points have been placed in particularly symmetrical position:  $[0, -\omega^j, 1]$ ,  $[1, 0, -\omega^j]$ , and  $[-\omega^j, 1, 0]$ ,  $j = 0, 1, 2$ . These are precisely the points in the image  $p(\Lambda)$  of the inflectional lattice.

By analyzing the symmetries of the so-called ‘tactical configuration’ of nine points and twelve lines containing them, one may determine which curves  $p_\lambda = 0$  are equivalent, and determine symmetries of a given such curve. Generically,  $|\text{Sym}(p_\lambda)| = 18$ , but the Fermat cubic  $p_0 = 0$  has three times as many symmetries because it is invariant under the transformations  $[X, Y, Z] \rightarrow [X, Y, \omega^j Z]$ . For details, see [3], pp. 291–297.

## 6. The Trihyperbola and Trefoil: A Reciprocal Pair

The trihyperbola  $\mathcal{H}$  has polar equation  $2r^3 \cos 3\theta = 1$ . This is a convenient scaling since  $z \in \mathcal{H}$  then satisfies  $|z^3 - 1| = |z|^3$ ; that is,  $\mathcal{H}$  is the locus of points in  $\mathbb{C}$  whose distance from the origin equals the geometric mean of the distances to three *foci*,  $1, \omega, \omega^2$ .

Squaring the above equation gives  $z^3 + \bar{z}^3 = 1$ . Or, replacing  $z, \bar{z}$  by the independent, *isotropic coordinates*,  $R = x + iy$ ,  $B = x - iy$ —in which  $x, y$  are now allowed

to be complex—we have  $R^3 + B^3 = 1$  as the equation of the complex curve  $\mathcal{H} \subset \mathbb{C}^2$ . In rectangular coordinates,  $x = \frac{R+B}{2}$ ,  $y = \frac{R-B}{2i}$ , the equation is  $2x^3 - 6xy^2 = 1$ .

A linear equivalence,  $(R, B) \leftrightarrow (x, y)$ , between  $\mathcal{H}$  and  $\mathcal{F}$  has just been given, and it follows that  $|\text{Sym}(\mathcal{H})| = 54$ ,  $\mathcal{H}$  is tiled by 18 equilateral triangles, etc. It is more interesting that these features persist also under *inversion* of  $\mathcal{H}$ —a ‘non-projective equivalence’.

In fact, the trefoil  $\mathcal{T}$  may be defined by the polar equation  $r^3 = 2 \cos 3\theta$ , in which the radius is the reciprocal of the radius for  $\mathcal{H}$ . Actually, inversion is described by  $z \mapsto 1/z$  (not  $1/\bar{z}$ ) and the resulting equation  $|z^3 - 1| = 1$  shows that the trefoil is the locus of points  $z \in \mathbb{C}$  the product of whose distances from the three foci  $(1, \omega, \omega^2)$  is 1.

The sextic equation  $R^3B^3 - R^3 - B^3 = 0$  is obtained for  $\mathcal{T} \subset \mathbb{C}^2$ ; in rectangular coordinates,  $0 = (x^2 + y^2)^3 + 2x(3y^2 - x^2)$ . Introducing homogeneous coordinates via  $R = \alpha U/W$ ,  $B = \alpha V/W$  gives

$$U^3V^3 + U^3W^3 + W^3V^3 = 0. \quad (6.1)$$

Again, the three coordinates may be arbitrarily permuted and multiplied by cube roots of unity  $\omega^j$ ; in particular,  $|\text{Sym}(\mathcal{T})| = 54$ .

To be more explicit about the operation of inversion  $\sigma$ , we write  $\sigma(R, B) = (\frac{1}{R}, \frac{1}{B})$ , or  $\sigma([U, V, W]) = [\frac{1}{U}, \frac{1}{V}, \frac{1}{W}] = [VW, UW, UV]$ . In the language of projective geometry, this is a *quadratic transformation* built on the fundamental triangle  $\Delta = \mathcal{I}\mathcal{J}\mathcal{K}$  which has vertices at the origin  $\mathcal{K} = [0, 0, 1]$  and the two ideal points known as *circular points*,  $\mathcal{I} = [1, 0, 0]$ ,  $\mathcal{J} = [0, 1, 0]$ . Note: In homogeneous rectangular coordinates  $[X, Y, Z]$ , the circular points are  $\mathcal{I} = [1, -i, 0]$  and  $\mathcal{J} = [1, i, 0]$ , so any circle  $X^2 + Y^2 + Z(aX + bY + cZ) = 0$  is seen to contain these points.

Observe that  $\sigma$  is well-defined, as a mapping on projective space, except at the vertices  $\mathcal{I}, \mathcal{J}, \mathcal{K}$ . On the complement of the fundamental triangle,  $UVW = 0$ ,  $\sigma$  defines an involution. On the other hand,  $\sigma$  collapses each edge of  $\Delta$  to its opposite point; for instance, the preimage of  $\mathcal{K}$  is the ideal line  $W = 0$ .

This explains the trefoil’s triple point at the origin; namely, the cubic  $\mathcal{H}$  has three ideal points (corresponding to its three asymptotes), and these three points are all sent to  $\mathcal{K}$  by  $\sigma$ . Likewise,  $\mathcal{H}$  intersects both of the lines  $U = 0$  and  $V = 0$  three times, and  $\sigma$  turns these into triple points at  $\mathcal{I}$  and  $\mathcal{J}$ . These account for all 9 singularities of  $\mathcal{T}$ , in accord with the Clebsch formula for the genus of a curve of degree  $n$  with  $\delta$  nodes and  $\kappa$  cusps:  $1 = g(\mathcal{T}) = \frac{(n-1)(n-2)}{2} - \delta - \kappa = 10 - 9 - 0$ . Here we already know that  $\mathcal{T}$  is an elliptic curve because inversion, though not a projective transformation, is a Riemann surface equivalence.

One can also see now why  $\mathcal{H}$  does not lose symmetry under inversion. Namely, since any  $M \in \text{Sym}(\mathcal{H})$  also preserves  $\Delta$ , it may be conjugated by  $\sigma$  to give a well-defined projective symmetry of  $\mathcal{T}$ ; in fact, writing  $M$  as a product of permutation and diagonal matrices  $M = PD$ , we have  $\sigma M \sigma = PD^{-1}$ .

Though the three curves  $\mathcal{F}, \mathcal{H}, \mathcal{T}$  have isomorphic symmetry groups,  $\text{Sym}(\mathcal{T})$  is arguably the most tangible. Instead of having to keep track of *nine* indistinguishable

inflection points (of  $\mathcal{F}$  or  $\mathcal{H}$ ), a symmetry of  $\mathcal{T}$  can be described in terms of what it does to the triple points  $\mathcal{I}, \mathcal{J}, \mathcal{K}$ .

We can picture both the ‘red circular point’  $\mathcal{J}$  and the ‘blue circular point’  $\mathcal{I}$  as looking like the triple point at the origin  $\mathcal{K}$ . Indeed, permutation matrices  $P \in \text{Sym}(\mathcal{T})$  permute the three points.

On the other hand, the symmetry  $[U, V, W] \mapsto [\alpha U, \alpha^{-1}V, W]$  fixes each triple point. This symmetry appears in the real,  $x, y$ -plane as rotation about the origin by  $2\pi/3$ , and evidently permutes the branches of  $\mathcal{K}$  cyclically. Since the branches of  $\mathcal{J}$  show up as foci of  $\mathcal{T}$  in Figure 1, it is graphically evident that the branches of  $\mathcal{J}$  are likewise permuted (the same holds for  $\mathcal{I}$ , which is ‘at infinity’ in this projection).

As Riemann surface automorphisms, neither of the symmetries just mentioned has a fixed point—they are translations in the elliptic curve  $\mathcal{T}$ . There are in fact several types of symmetries with fixed points; these will be described further in connection with arc length parameterization of  $\mathcal{T}$ .

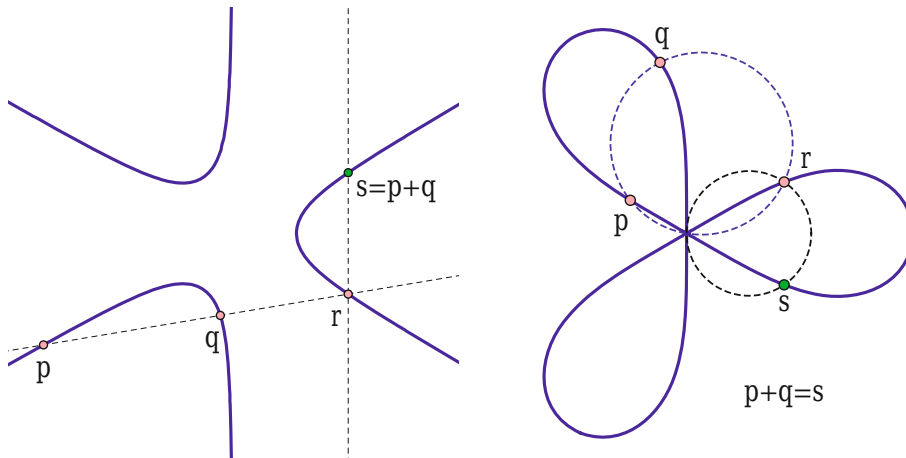


FIGURE 7. Addition on the cubic  $\mathcal{H}$  and sextic  $\mathcal{T} = \sigma(\mathcal{H})$ .

*Remark 6.1.* The real locus of  $\mathcal{T}$ , being compact, has further graphical advantages. For instance, the geometric addition law for (real) points on the elliptic curve  $\mathcal{T}$  takes place in a bounded region ( $|z| \leq 2^{1/3}$ ).

First, consider a pair of points  $p, q \in \mathcal{H}$ , and let  $L$  be the line containing both. Then the point  $r$  satisfying  $p + q + r = 0$  under addition on  $\mathcal{H}$  is determined geometrically as the third point of  $L \cap \mathcal{H}$ ; see Figure 7. Next, to determine  $s = p + q$ , we need to define the operation  $r \mapsto -r$ . This requires fixing an ‘origin’  $o \in \mathcal{H}$ ; a natural choice is the ideal point  $o = [X, Y, Z] = [0, 1, 0]$  corresponding to the vertical asymptote. Then the vertical line  $\overline{o r}$  intersects  $\mathcal{H}$  at  $-r = s$ .

Now  $\sigma$  preserves addition as it transforms the entire construction from left to right in Figure 7:  $\sigma(\mathcal{H}) = \mathcal{T}$ ,  $\sigma(L) = C$ , a circle through the origin  $\mathcal{K} = \sigma(o)$ , and  $\sigma(\overline{o r}) = C_0$ , a circle tangent to  $\overline{o r}$  at  $\mathcal{K}$ . We note that, by Bezout’s Theorem,  $C$  intersects  $\mathcal{T}$  a total of  $6 \times 2 = 12$  times. The triple points at the origin and two

circular points count for  $3 \times 3 = 9$  points (generically); the remaining 3 points are labelled  $p, q, r$  in the figure. The count for  $C_0$  is similar, but  $C_0$  meets  $\mathcal{H}$  four times at  $\mathcal{K}$ , so there are only two additional finite points  $r, s$ .

To summarize: Given  $p, q \in \mathcal{T}$ , find  $r$  as the ‘twelfth’ intersection of  $\mathcal{T}$  with the circle through  $p, q$ , and the origin; then find  $s$  as the ‘twelfth’ intersection with the tangent circle  $C_0$  through  $r$ .

### 7. Parameterization of $\mathcal{T}$

Isotropic coordinate functions  $R = \text{cm } z$  and  $B = \text{sm } z$  parameterize the trihyperbola  $R^3 + B^3 = 1$ ; correspondingly,  $R(z) = 1/\text{cm } z$ ,  $B(z) = 1/\text{sm } z$  parameterize the trefoil  $R^3 + B^3 = R^3 B^3$ . Unfortunately, these do not yield real points for  $z = u \in \mathbb{R}$  (e.g., for  $u = 0$ ).

Yet the latter parameterization satisfies a most fortuitous equation:  $x'^2 + y'^2 = R'B' = \frac{B^2}{R^2} \cdot \frac{-R^2}{B^2} = -1$ . Better yet,  $R(z) = 1/\text{cm } iz$  and  $B(z) = 1/\text{sm } iz$  parameterize  $\mathcal{T}$  and satisfy the ‘unit speed condition’  $R'B' = 1$ —whatever that means!

In fact, we are but a step away from an arc length parameterization of the real trefoil. But first, it will be useful to introduce ‘twisted’ Dixon functions:

$$S(z) = \text{sm } iz, \quad C(z) = \text{cm } iz \tag{7.1}$$

Then Equation 2.5 gives at once  $S(\omega z) = \omega S(z)$ ,  $C(\omega z) = C(z)$  and

$$S(\alpha z) = \frac{\alpha S(z)}{C(z)}, \quad C(\alpha z) = \frac{1}{C(z)} \tag{7.2}$$

follow likewise from Equation 3.2.

For translational identities, it will be convenient to use the basis

$$e_1 = K/\beta, \quad e_2 = \beta K, \quad \beta = e^{i\pi/6} \tag{7.3}$$

and to adopt the following variants of earlier notations:

$$\Lambda' = \{m e_1 + n e_2\}, \quad \Pi' = \{m 3e_1 + n 3e_2\}, \quad \Sigma' = \mathbb{C}/\Pi' \tag{7.4}$$

The corresponding Platonic surface  $\Sigma'_{18}$  is represented in Figure 8, as a triangulated rhombus spanned by  $3e_1$  and  $3e_2$ , with opposite edges identified. The color-coding for points in  $\Lambda'$  will be explained shortly.

The following identities are now easily derived:

$$S(z + e_1) = -\frac{\omega C(z)}{S(z)}, \quad S(z + e_2) = \frac{\omega}{C(z)} \tag{7.5}$$

$$C(z + e_1) = \frac{\omega^2}{S(z)}, \quad C(z + e_2) = -\frac{\omega^2 S(z)}{C(z)} \tag{7.6}$$

Using  $\sqrt{3}K = e_1 + e_2$ , these yield quasi-period identities

$$S(z + \sqrt{3}K) = \omega^2 S(z), \quad C(z + \sqrt{3}K) = \omega C(z), \tag{7.7}$$

which will shortly acquire a simple geometric interpretation.

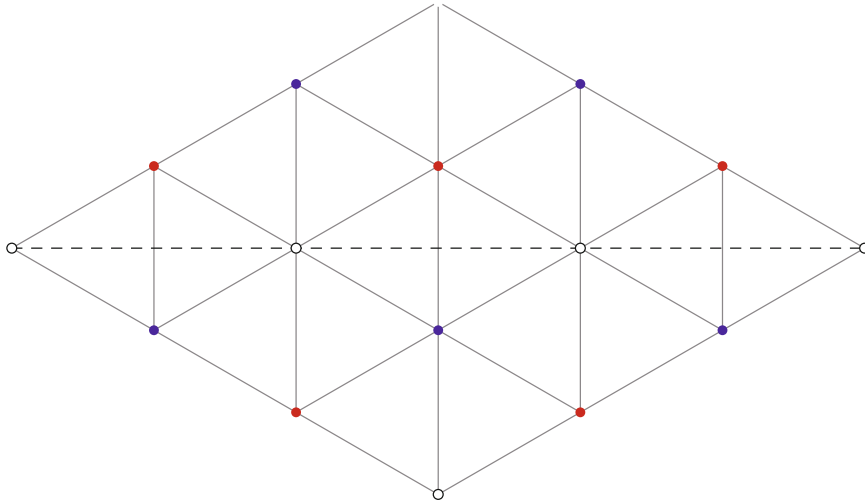


FIGURE 8. The Platonic surface  $\Sigma'_{18}$ ; pre-images of triple points (red, white, blue), and real locus (dashed) of  $\mathcal{T}$ .

Returning to the parameterization of  $\mathcal{T}$ , we note that Equations 7.5, 7.6 may be used with  $iK = \omega e_1$  to obtain

$$S(z + iK) = -\frac{C(z)}{S(z)}, \quad C(z + iK) = \frac{1}{S(z)}. \tag{7.8}$$

Therefore, the substitution  $z \rightarrow z + iK$  turns the previous  $R, B$  into:

$$R(z) = S(z), \quad B(z) = -\frac{S(z)}{C(z)} = S(-z) \tag{7.9}$$

Since we have merely translated the parameter, the equations  $R^3 + B^3 = R^3 B^3$  and  $R'B' = 1$  continue to hold; but now  $R(0) = B(0) = 0$  and, more generally,  $u \in \mathbb{R}$  is mapped by  $p = (R, B)$  to a real point of  $\mathcal{T}$ . Thus, we have obtained the promised parameterization  $p : \Sigma' \rightarrow \mathcal{T}$ . (Expressions for the corresponding  $x, y$  coordinates are given in §10.)

Referring to Figure 8 as a model of the domain of  $p$ , we note that white, red, and blue dots denote pre-images of the three triple points; respectively, the origin  $\mathcal{K}$ , the red circular point  $\mathcal{J}$  and the blue circular point  $\mathcal{I}$ . Also, the real axis is the pre-image of the real locus of  $\mathcal{T}$ . In other words, for  $s$  real,  $R(s) = S(s)$  traces the real trefoil curve in the Gaussian plane. The quasi-period relation  $S(z + \sqrt{3}K) = \omega^2 S(z)$  therefore expresses the 3-fold rotational symmetry of the real curve.

*Remark 7.1.* Since  $p$  was just obtained in a rather *ad hoc* manner, let us now reconsider arc length parameterization of a curve by first principles. If  $G(R, B) = 0$  is the equation for a curve in isotropic coordinates, then the arc length element may be expressed

$$ds^2 = dRdB = -\frac{G_R}{G_B}dR^2 = -\frac{G_B}{G_R}dB^2 \tag{7.10}$$

In the case of the trefoil,  $G(R, B) = \frac{1}{R^3} + \frac{1}{B^3} - 1$  gives  $ds^2 = -\frac{B^4}{R^4}dR^2$ . We may solve for  $\frac{dR}{ds} = R' = 1/B'$ , making a choice of sign. Assuming  $p(0) = (0, 0)$ , the ‘half way point’ is the trefoil’s intersection with the positive real axis,  $p(3\sqrt{3}K/2) = (\sqrt[3]{2}, \sqrt[3]{2})$ . Then  $p = (R, B)$  is uniquely determined by the following initial value problem:

$$\frac{dR}{ds} = -i\frac{B^2}{R^2}, \quad \frac{dB}{ds} = i\frac{R^2}{B^2} \tag{7.11}$$

$$R(3\sqrt{3}K/2) = B(3\sqrt{3}K/2) = \sqrt[3]{2} \tag{7.12}$$

Of course, the solution  $p(s)$  also satisfies  $p(0) = (0, 0)$ , but this is not *a priori* valid as initial condition.

### 8. Projective symmetries of $p : \Sigma' \rightarrow \mathcal{T}$

To discuss equivariance of  $p : \Sigma' \rightarrow \mathcal{T}$ , we re-express  $p$  in homogeneous coordinates satisfying Equation 6.1:

$$p = [U, V, W] = [R, B, \alpha] = [S, -\frac{S}{C}, \alpha] \tag{8.1}$$

The symmetries in the  $z$ -plane may be generated by  $\frac{\pi}{3}$ -rotation  $A(z) = \alpha z$  and the translation  $E_1(z) = z + e_1$ . Equations 7.2, 7.5, 7.6 give:

$$A^*p = [\frac{\alpha S}{C}, -\alpha S, \alpha] = [-\omega^2\frac{S}{C}, \omega^2 S, \alpha] = [\omega^2 V, \omega^2 U, W],$$

$$E_1^*p = [-\frac{\omega C}{S}, \omega^2 C, \alpha] = [-\omega, \omega^2 S, \alpha\frac{S}{C}] = [\alpha, S, -\frac{S}{C}] = [W, U, V].$$

It follows that  $p : \Sigma' \rightarrow \mathcal{T}$  is equivariant with respect to the 54-element symmetry groups  $\text{Aut}(\Sigma'_{18})$  and  $\text{Sym}(\mathcal{T})$ .

Details of the correspondence  $\text{Aut}(\Sigma'_{18}) \xleftrightarrow{p} \text{Sym}(\mathcal{T})$  are of interest and merit systematic discussion.

To begin, note that elements of  $\text{Aut}(\Sigma'_{18})$  are induced by orientation-preserving *wallpaper symmetries*—that is, affine maps  $w = f(z) = az + b$  which preserve the lattice  $\Lambda$ . These are: Translations generated by  $E_1, E_2$ ; rotations about a lattice point by a multiple of  $\pi/3$ ; rotations by  $\pm 2\pi/3$  about a *tile centroid*;  $\pi$ -rotations about an *edge midpoint*.

To discuss the various trefoil symmetries we now proceed to: a) Give representative affine maps  $f$ ; b) Identify fixed points of the induced automorphisms  $\phi \in \text{Aut}(\Sigma'_{18})$ ; c) Describe the corresponding projective symmetries  $F \in \text{Sym}(\mathcal{T})$ . It will be useful to refer to Figure 8.

1.  $\mathbf{f}_{jk} = \mathbf{E}_1^j \mathbf{E}_2^k$ : Lattice translations  $f_{jk}$  induce torus translations  $\phi_{jk}$ ,  $0 \leq j, k \leq 2$ , which fix no points ( $\phi_{jk} \neq \text{Id}$ ). As the figure shows (and as verified above),  $f_{10} = E_1$  corresponds to a projective transformation  $F_{10}$  which cyclically permutes triple points (likewise  $F_{01}$ ); on the other hand,  $F_{11}$  preserves triple points but cyclically permutes their branches.

2. **f = A** : One may picture the fixed point  $z_0 = 0$ , say, as the second white point from the left. (To see that  $\phi_A$  has just the one fixed point, one may rearrange the tiles to form a hexagon with center  $z_0 = 0$ .)

$F[U, V, W] = [V, U, \omega W]$  swaps  $\mathcal{I}$  and  $\mathcal{J}$  and swaps two of the three branches of  $\mathcal{K}$ . The tangent lines to  $\mathcal{T}$  at  $\mathcal{K}$  have equation  $0 = U^3 + V^3 = (U + V)(U + \omega V)(U + \omega^2 V)$ . The vertical tangent  $2x = (U + V) = 0$  is preserved, and the corresponding branch of  $\mathcal{K} = [0, 0, 1]$  is the unique fixed point  $p(0) \in \mathcal{T}$ .

3. **f = A<sup>2</sup>** : The rotation  $f(z) = \omega z$  induces an automorphism  $\phi = \phi_A^2$  which fixes the three ‘white points’,  $0, \sqrt{3}K, 2\sqrt{3}K \in \Sigma'_{18}$ , and  $F^2[U, V, W] = [U, V, \omega^2 W]$  takes each branch  $p(0), p(\sqrt{3}K), p(2\sqrt{3}K)$  of  $\mathcal{K}$  to itself but ‘spins’ each tangent line  $U + \omega^j V = 0$  about  $\mathcal{K}$  by multiplication of its points by  $\omega$ .
4. **f = A<sup>3</sup>** :  $fz = -z$  induces the ‘standard torus involution’ with *four* fixed points. If  $z_0 = 0$  is the leftmost white point,  $\phi = \phi_A^3$  may be pictured, alternatively, as  $\pi$ -rotation about the central point in the rhombus,  $z_1 = 3\sqrt{3}K/2$ ; the other two fixed points are the ‘semi-periods’  $3e_1/2, 3e_2/2 \in \Sigma'_{18}$ .

$F^3[U, V, W] = [V, U, W]$  swaps  $\mathcal{I}$  and  $\mathcal{J}$  and swaps two of the three branches of  $\mathcal{K}$ . Each involution in  $\text{Sym}(\mathcal{T})$  is conjugate to this one. In particular, it would now be redundant to consider  $\pi$ -rotation about an edge midpoint!

5. **f = B** :  $Bz = \omega z + e_1 = \omega z + \frac{1-\omega}{\sqrt{3}}K$  is rotation about the tile centroid  $z_2 = K/\sqrt{3}$ . The induced map  $\phi_B$  fixes also  $z_2 + \sqrt{3}K$  and  $z_2 + 2\sqrt{3}K \in \Sigma'_{18}$ .  $F_B[U, V, W] = E_1 A^2[U, V, W] = [\omega^2 W, U, V]$  permutes triple points cyclically.

*Remark 8.1.* The last two entries represent a point of contact between symmetry and uniform subdivision of  $\mathcal{T}$ . Namely,  $p(z_1) = [\sqrt[3]{2}, \sqrt[3]{2}, \alpha]$  bisects a leaf of the trefoil (see Equation 7.12), while  $p(z_2)$  and  $p(2z_2)$  trisect a leaf of  $\mathcal{T}$ .

By the theory of subdivision, the latter points must also be given by values of the transcendental function  $\text{sm } x$  expressible via square roots and cube roots. In fact,  $p(z_2) = [e^{5\pi i/9}, e^{-5\pi i/9}, \alpha]$  may be characterized algebraically as a fixed point of  $F_B$ ; alternatively,  $p(z_2)$  is the first intersection of  $p(x)$  with the unit circle (see Figure 1).

## 9. Reflections and Riemannian symmetries of $\mathcal{T}$

The theory of Platonic surfaces encompasses anti-holomorphic as well as holomorphic symmetries of Riemann surfaces. In the present case, the full group of 108 symmetries  $\text{Aut}_{\pm}(\Sigma'_{18})$  is generated by anti-holomorphic reflections in the three edges of a small, 30-60-90-triangle  $\tau \subset \mathbb{C}$  with one vertex of each type considered above; say,  $z_0 = 0, z_2 = K/\sqrt{3}$  and  $z'_1 = e_2/2$ . Alternatively,  $\text{Aut}_{\pm}(\Sigma'_{18})$  is generated by the subgroup  $\text{Aut}(\Sigma'_{18})$  (‘reflection pairs’) together with a single reflection—say, reflection across edge  $z_0 z_2$ , i.e., complex conjugation.

Each reflection  $\phi \in \text{Aut}_{\pm}(\Sigma'_{18})$  has a line  $L_{\phi}$  as fixed point set, and the set of all such lines give the barycentric subdivision of  $\Sigma'_{18}$ . The 108 triangles of the resulting Platonic surface  $\Sigma'_{108}$  are permuted simply transitively by  $\text{Aut}_{\pm}(\Sigma'_{108}) = \text{Aut}_{\pm}(\Sigma'_{18})$ .

(The equivalent Platonic surface  $\Sigma_{108}$  is modeled by the central trihexagon in Figure 4.)

Since the trefoil parameterization  $p$  preserves reality, a corresponding group  $\text{Sym}_{\pm}(\mathcal{T})$  may be generated by the projective trefoil symmetries  $\text{Sym}(\mathcal{T})$ , together the canonical involution on  $\mathbb{C}\mathbb{P}^2$  given by complex conjugation of rectangular coordinates  $[X, Y, Z] \mapsto [\bar{X}, \bar{Y}, \bar{Z}]$ ; this induces ‘reflection of  $\mathcal{T}$  in its real locus’ (the *real structure* of  $\mathcal{T}$ ).

We recapitulate the results of the last several sections on trefoil parameterization and symmetry:

- Theorem 9.1.**
- i) *Arc length parameterization of the trefoil  $p : \mathbb{R} \rightarrow \mathcal{T}$  is given in isotropic coordinates  $p = (R, B)$  via the Dixon sine function by  $p(s) = (\text{sm } is, \text{sm } -is)$ ; this uniquely solves Equations 7.11, 7.12.*
  - ii) *By analytic continuation and projective completion,  $p$  extends to an unbranched covering  $p : \mathbb{C} \rightarrow \mathcal{T} \subset \mathbb{C}\mathbb{P}^2$  with period lattice  $\Pi'$  (See 7.4). The induced map on the quotient  $\Sigma' = \mathbb{C}/\Pi'$  is 1-1 except that  $p : \Sigma' \rightarrow \mathcal{T}$  maps the nine vertices of  $\Sigma'_{18}$  to the trefoil’s three triple points. Thus,  $p$  uniformizes  $\mathcal{T}$  as an elliptic curve.*
  - iii)  *$p : \Sigma'_{108} \rightarrow \mathcal{T}$  is an isomorphism of Platonic surfaces: To each  $\phi \in \text{Aut}_{\pm}(\Sigma'_{108})$ , there corresponds a unique symmetry  $F \in \text{Sym}_{\pm}(\mathcal{T})$  satisfying  $Fp = p\phi$ , and the 108 faces of the trefoil  $\mathcal{T}_{108} = p(\Sigma'_{108})$  are thereby permuted, simply transitively, by  $\text{Sym}_{\pm}(\mathcal{T}) \simeq \text{Aut}_{\pm}(\Sigma'_{108})$ .*

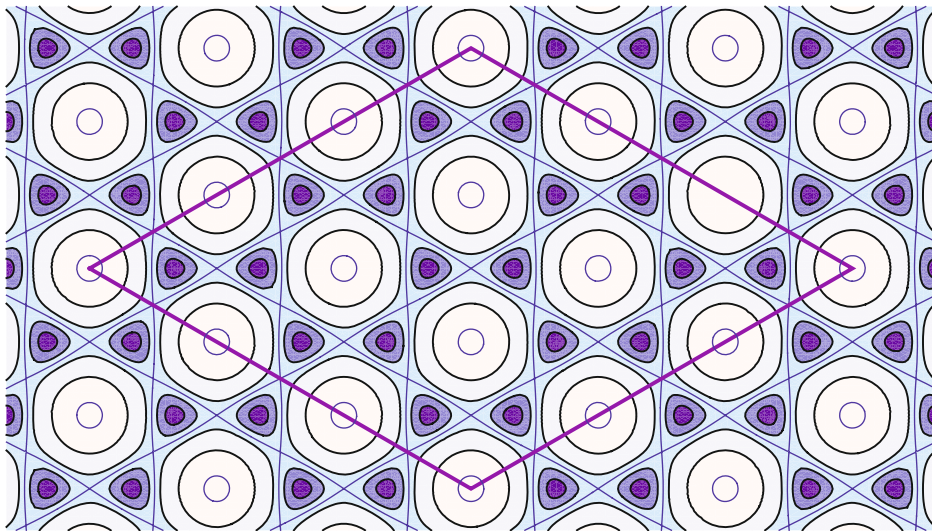


FIGURE 9. Level sets of Gauss curvature ( $p^*G$ ) of the trefoil.

*Remark 9.2.* The fit between intrinsic and extrinsic symmetry of  $\mathcal{T} \subset \mathbb{C}\mathbb{P}^2$  may be further illuminated by considering the *Fubini-Study* metric  $g$  on  $\mathbb{C}\mathbb{P}^2$  [19]. For

$g$ -symmetry, the scaling  $A = \sqrt{8}$  is required in the original equation for  $\mathcal{T}$ . Then the induced Riemannian metric on the trefoil, though no longer flat, turns out to have the same group of 108 Riemannian symmetries. Further, the edges of  $\mathcal{T}_{108}$  again belong to geodesics, namely, fixed point sets of isometric reflections. (Details are discussed for the lemniscate in [15].)

The Gaussian curvature  $G : \mathcal{T} \rightarrow \mathbb{R}$  of such a metric must have (at least) 54 critical points corresponding to the vertices of  $\mathcal{T}_{108}$  since these are fixed points of orientation-preserving isometries. Figure 9 shows a level set diagram of the pulled-back curvature  $p^*G$  which suggests that  $G$  has *precisely* 54 critical points. Then  $G$  has just the critical values:  $G_{\max} = G(p(0)) = 2$ ,  $G_{\min} = G(p(K/\sqrt{3})) = -14$ , and

$$G_{\text{saddle}} = G(p(z_1)) = G([\sqrt[3]{2}, \sqrt[3]{2}, \alpha]) = 2 - 4\sqrt[3]{2} \approx -3.04$$

The precise value for  $G_{\text{saddle}}$  is useful for plotting the saddle level set of  $p^*G$ —which apparently consists of nearly straight lines!

### 10. Appendix

All required identities for  $\text{sm } z$  and  $\text{cm } z$  may be recovered from the fundamental addition and subtraction formulas (see [2], pp. 13–14, or [9], pp. 179–180). Using the shorthand  $s_1 = \text{sm } u$ ,  $s_2 = \text{sm } v$ ,  $c_1 = \text{cm } u$ ,  $c_2 = \text{cm } v$ , the formulas are:

$$\begin{aligned} \text{sm}(u + v) &= \frac{s_1^2 c_2 - s_2^2 c_1}{s_1 c_2^2 - s_2 c_1^2} = \frac{s_1 + s_2 c_2 c_1^2}{c_2 + s_1 c_1 s_2^2} \\ \text{cm}(u + v) &= \frac{s_1 c_1 - s_2 c_2}{s_1 c_2^2 - s_2 c_1^2} = \frac{c_1 c_2^2 - s_1^2 s_2}{c_2 + s_1 c_1 s_2^2} \\ \text{sm}(u - v) &= \frac{s_1^2 c_2 - s_2^2 c_1}{s_1 + s_2 c_2 c_1^2} = \frac{s_1 c_1 - s_2 c_2}{c_1 c_2^2 - s_1^2 s_2} \\ \text{cm}(u - v) &= \frac{s_2 + s_1 c_1 c_2^2}{s_1 + s_2 c_2 c_1^2} = \frac{c_2 c_1^2 - s_2^2 s_1}{c_1 c_2^2 - s_1^2 s_2} \end{aligned}$$

For instance, setting  $u = z$ ,  $v = \omega^j K$ , the first two equations give Equation 3.1. Likewise, with  $u = 0$ ,  $v = z$ , the third and fourth equations give Equation 3.3. This in turn gives Equation 3.2, using  $\alpha z = -\omega^2 z$  and Equation 2.5.

It is also useful to be able to express  $S(z) = \text{sm } iz$ ,  $C(z) = \text{cm } iz$  in terms of  $\text{sm } z$ ,  $\text{cm } z$ . Using the identity  $i = \frac{\omega - \omega^2}{\sqrt{3}}$ , and letting  $v = \frac{u}{\sqrt{3}}$ , the subtraction formulas give:

$$\text{sm } iu = \frac{\sqrt{3}i \text{sm } v \text{cm } v}{\text{cm}^3 v - \omega \text{sm}^3 v}, \quad \text{cm } iu = \frac{\text{cm}^3 v - \omega^2 \text{sm}^3 v}{\text{cm}^3 v - \omega \text{sm}^3 v} \tag{10.1}$$

We can now express the trefoil parameterization 7.9 in rectangular coordinates  $x$ ,  $y$ . Using the shorthand  $\sigma = \text{sm } \frac{s}{\sqrt{3}}$ ,  $c = \text{cm } \frac{s}{\sqrt{3}}$ :

$$\begin{aligned}
 x(s) &= \frac{R(s) + B(s)}{2} = \frac{S(s)(C(s) - 1)}{2C(s)} = \frac{i\sqrt{3}\sigma c}{2(c^3 - \omega^2\sigma^3)} \cdot \frac{(\omega - \omega^2)\sigma^3}{c^3 - \omega\sigma^3} \\
 &= -\frac{3\sigma^4 c}{2(c^6 + \sigma^6 + \sigma^3 c^3)} = -\frac{3\sigma^4 c}{2(1 - \sigma^3 c^3)}, \\
 y(s) &= \frac{R(s) - B(s)}{2i} = \frac{S(s)(C(s) + 1)}{2iC(s)} = \frac{\sqrt{3}\sigma c}{2(c^3 - \omega^2\sigma^3)} \cdot \frac{2c^3 - (\omega + \omega^2)\sigma^3}{c^3 - \omega\sigma^3} \\
 &= \frac{\sqrt{3}\sigma c(2 - \sigma^3)}{2(c^6 + \sigma^6 + \sigma^3 c^3)} = \frac{\sqrt{3}\sigma c(1 + c^3)}{2(1 - \sigma^3 c^3)}.
 \end{aligned}$$

Incidentally, these formulas lead to  $r^2 = x^2 + y^2 = \frac{3\sigma^2 c^2}{1 - \sigma^3 c^3}$ .

To conclude this appendix, we note that Dixon functions are not built into the software package *Mathematica*, which was used to generate figures in this paper. For purposes of numerical computation, it is quite useful to know that these functions may be expressed in terms of ‘standard’ functions.

To quote formulas involving the Weierstrass  $\wp$ -function, we recall that this function satisfies a differential equation of the form  $\wp'^2 = 4\wp^3 - g_2\wp - g_3 = 4(\wp - e_1)(\wp - e_2)(\wp - e_3)$ . Here, the critical values of  $\wp$  are distinct:  $0 \neq [4(e_1 - e_2)(e_2 - e_3)(e_3 - e_1)]^2 = g_2^3 - 27g_3^2$ . The most symmetrical cases correspond to one or the other of  $g_2, g_3$  vanishing. (By scaling, the remaining coefficient can be normalized to 1.) In these two cases only, the quantity  $\lambda = \frac{e_3 - e_2}{e_1 - e_2}$  yields fewer than *six* distinct values under permutation of  $e_j$ . (See [1], Ch. 7, for an introduction to elliptic functions and the Weierstrass theory.)

In fact,  $g_3 = 0$  is the *harmonic* (or *lemniscate*) case (three  $\lambda$ -values), which corresponds to a square period lattice. The most symmetric case of all,  $g_2 = 0$ , is the *equianharmonic* case (two  $\lambda$ -values), which is the hexagonal case of the Dixon functions with  $a = 0$ .

For present purposes, a convenient normalization is  $g_2 = 0$ ,  $g_3 = \frac{1}{27}$ . Using this case of the Weierstrass  $\wp$ -function,  $\text{sm } z$  and  $\text{cm } z$  may be expressed:

$$\text{sm } z = \frac{6\wp(z)}{1 - 3\wp'(z)}, \quad \text{cm } z = \frac{3\wp'(z) + 1}{3\wp'(z) - 1}$$

In [7], p.39, these formulas are attributed to Dumont [10].

Elegant as these formulas may be, they still require some care to apply. For instance, *Mathematica* reports division by zero when one uses these formulas to parametrically plot  $\mathcal{T}$  as  $p(s) = (\Re[\text{sm } is], \Im[\text{sm } is])$ ,  $0 \leq s \leq 3\sqrt{3}K$ . Note that although  $p(t)$  should be well-behaved at  $t = 0$ , the Weierstrass function itself has a second order pole at the origin.

## References

- [1] Lars Ahlfors, *Complex Analysis*, Second Edition, McGraw-Hill, 1966.

- [2] Oscar S. Adams, *Elliptic Functions Applied to Conformal World Maps*, U.S. Coast and Geodetic Survey Special Publ. No.112, Washington, 1925.
- [3] E. Brieskorn and H. Knörrer, *Plane Algebraic Curves*, Birkhäuser, 1986.
- [4] Annalisa Calini and Joel Langer, Schwarz reflection geometry I: continuous iteration of reflection, *Math. Z.*, **244** (2003) pp. 775–804.
- [5] ———, *Schwarz reflection geometry II: local and global behavior of the exponential map*, *Exp. Math.*, **16** (2007), No. 3, pp. 321–346.
- [6] Arthur Cayley, Reduction of  $\int \frac{dx}{(1-x^3)^{2/3}}$  to elliptic integrals, *Messenger of Mathematics XI*, (1882) 142–143, reprinted in *Collected Mathematical Papers*.
- [7] Eric Conrad and Philippe Flajolet, The Fermat cubic, elliptic functions, continued fractions, and a combinatorial excursion, *Séminaire Lotharingien de Combinatoire (SLC)* **54** (2006), 44 pages.
- [8] David Cox and Jerry Shurman, Geometry and number theory on clovers, *Amer. Math. Monthly*, **112** (2005), 682–704.
- [9] A. C. Dixon, On the doubly periodic functions arising out of the curve  $x^3+y^3-3axy=1$ , *Quart. Journal Pure. Appl. Math.*, **24** (1890), 167–233.
- [10] Dominique Dumont, Le paramétrage de la courbe d'équation  $x^3+y^3=1$ , Manuscript (1988), 18 pages.
- [11] Maxim Hendriks, Platonic maps of low genus, Thesis, Technische Universiteit Eindhoven, 2013.
- [12] Joel Langer, On meromorphic parametrizations of real algebraic curves, *J. Geom.*, **100**, No. 1 (2011), 105–128.
- [13] Joel Langer and David Singer, Foci and foliations of real algebraic curves, *Milan J. Math.*, **75** (2007), 225–271.
- [14] ———, When is a curve an octahedron?, *Amer. Math. Monthly*, **117**, No. 10 (2010), 889–902.
- [15] ———, Reflections on the lemniscate of Bernoulli: The forty eight faces of a mathematical gem, *Milan J. Math.*, Vol 78 (2010), 643–682.
- [16] ———, The lemniscatic chessboard, *Forum Geometricorum*, Vol. 11 (2011), 183–199.
- [17] ———, Subdividing the trefoil by origami, *Geometry*, Vol. 2013, ID 897320.
- [18] ———, Singularly beautiful curves and their elliptic curve families, in preparation.
- [19] Linda Ness, Curvature on algebraic plane curves. I, *Compositio Mathematica* **35** (1977), pp. 57–63.
- [20] Michael Rosen, Abel's theorem on the lemniscate, *Amer. Math. Monthly*, **88** (1981), 387–395.
- [21] Victor Prasolov and Yuri Solovyev, *Elliptic Functions and Elliptic Integrals*, Translations of Mathematical Monographs, Vol. 170, American Mathematical Society, Providence, 1997.
- [22] Cornelis Zwikker, *The Advanced Geometry of Plane Curves and Their Applications*, Dover, New York, 2005.

Joel C. Langer  
Dept. of Mathematics  
Case Western Reserve University  
Cleveland, OH 44106-7058  
USA  
e-mail: [joel.langer@case.edu](mailto:joel.langer@case.edu)

David A. Singer  
Dept. of Mathematics  
Case Western Reserve University  
Cleveland, OH 44106-7058  
USA  
e-mail: [david.singer@case.edu](mailto:david.singer@case.edu)

Received: August 8, 2013.